Chapter 3

Full Vehicle Simulation Model

Two different versions of the full vehicle simulation model of the test vehicle will now be described. The models are validated against experimental results. A unique steering driver model is proposed and successfully implemented. This driver model makes use of a non-linear gain, modelled with the Magic Formula, traditionally used for the modelling of tyre characteristics.

3.1 Initial Vehicle Model

A Land Rover Defender 110 was initially modelled in ADAMS View 12 (MSC 2005) with standard suspension settings as a baseline. The ADAMS 521 interpolation tyre model is used, because of its ability to incorporate test data in table format. The tyre's vertical dynamics and load dependent lateral dynamics are thus considered in this model. In order to keep the model as simple as possible, yet as complex as necessary, longitudinal dynamic behaviour of the tyres and vehicle is not considered here. The anti-roll bar and bump stops are left unchanged. Only the spring and damper characteristics are changed for optimisation purposes. This study builds on current research into a two-state semi-active spring-damper system. The semi-active unit has been included in the ADAMS model and replaces the standard springs and dampers. The inertias of the vehicle body were determined by scaling down data available for an armoured prototype Land Rover 110 Wagon, and were considered to be representative of the lighter vehicle.

The complete model consists of 16 unconstrained degrees of freedom, 23 moving parts, 11 spherical joints, 10 revolute joints, 9 Hooke's joints, and one motion defined by the steering driver. The vehicle direction of heading is controlled by a simple single point steering driver, adjusting the steering wheel rotation according to the difference of the desired course from the current course at a preview distance ahead of the vehicle.

3.2 Refined Vehicle Model

A refined model of the Land Rover Defender 110 is also modelled in MSC.ADAMS View (MSC 2005) with standard suspension settings, as a baseline. For this model, the non-linear MSC.ADAMS Pacejka 89 tyre model (Bakker et al. 1989) is fitted to measured tyre data, and used within the model. This tyre model was selected as it was found that the 5.2.1 tyre model could not handle tyre slip angles larger than 3 degrees. The Pacejka 89 tyre model was used with a point follower approximation for rough terrain, to speed up the simulation speed, and as a result of limited tyre and test track data available at the time. As in the initial model, the tyre's vertical dynamics and load dependent lateral dynamics are also considered in this model. In order to keep the model as simple as possible, yet as complex as necessary, longitudinal dynamic behaviour of the tyres and vehicle is again not considered here. The vehicle body is modelled as two rigid bodies connected along the roll axis at the chassis height, by a revolute joint and a torsional spring, in order to better capture the vehicle dynamics due to body torsion in roll. The anti-roll bar is modelled as a torsional spring between the two rear trailing arms to be representative of the actual anti-roll bar's effect. The bump and rebound stops, are modelled with non-linear splines, as force elements between the axles and vehicle body. The suspension bushings are modelled as kinematic joints with torsional spring characteristics that are representative of the actual vehicle's suspension joint characteristics, in an effort to speed up the solution time, and help decrease numerical noise. The baseline vehicle's springs and dampers are modelled

Table 3.1: MSC.ADAMS vehicle model's degrees of freedom

Body	Degrees of Freedom	Associated Motions
Vehicle Body	7	body torsion
(2 rigid bodies)		longitudinal, lateral, vertical
		roll, pitch, yaw
Front Axle	2	roll, vertical
Rear Axle	2	roll, vertical
Wheels	4 x 1	rotation

with measured non-linear splines. The vehicle's center of gravity (cg) height and moments of inertia were measured (Uys et al. 2005) and used within the model. Only the spring and damper characteristics are changed for optimisation purposes. The $4S_4$ unit has been included in the MSC.ADAMS model, using the MSC.ADAMS Controls environment to include the Simulink model, and replaces the standard springs and dampers. Due to the fact that different suspension characteristics are being included the first two seconds of the simulation have to be discarded, while the vehicle is settling into an equilibrium condition. Figures 3.1 and 3.2 indicates the detailed kinematic modelling of the rear and front suspensions. The complete model consists of 15 unconstrained degrees of freedom, 16 moving parts, 6 spherical joints, 8 revolute joints, 7 Hooke's joints, and one motion defined by the steering driver. The degrees of freedom are indicated in Table 3.1.

The vehicle's direction of heading is controlled by a carefully tuned yaw rate steering driver, adjusting the front wheels' steering angles according to the difference of the desired course from the current course at a preview distance ahead of the vehicle (see paragraph 3.4). The longitudinal driver is modelled as a variable force attached to the body at wheel height depending on the difference between the instantaneous speed and desired speed (see paragraph 3.3). This MSC.ADAMS model is linked to MATLAB (Mathworks 2000b) through a Simulink block that requires as inputs the spring and damper design variable values, and returns outputs of vertical accelerations, vehicle body roll angle and roll velocity.

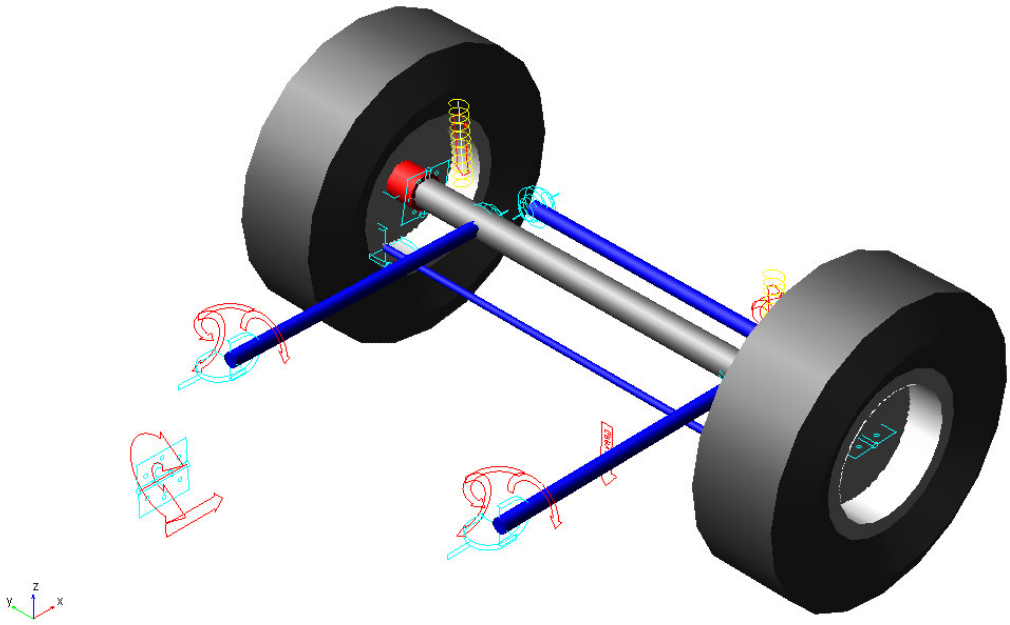

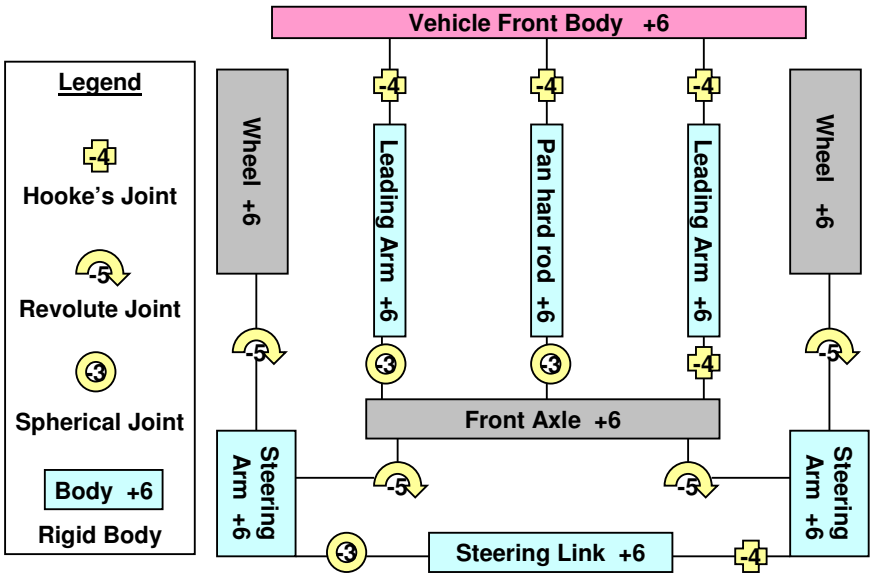

Figure 3.1: Modelling of the full vehicle in MSC.ADAMS, front suspension

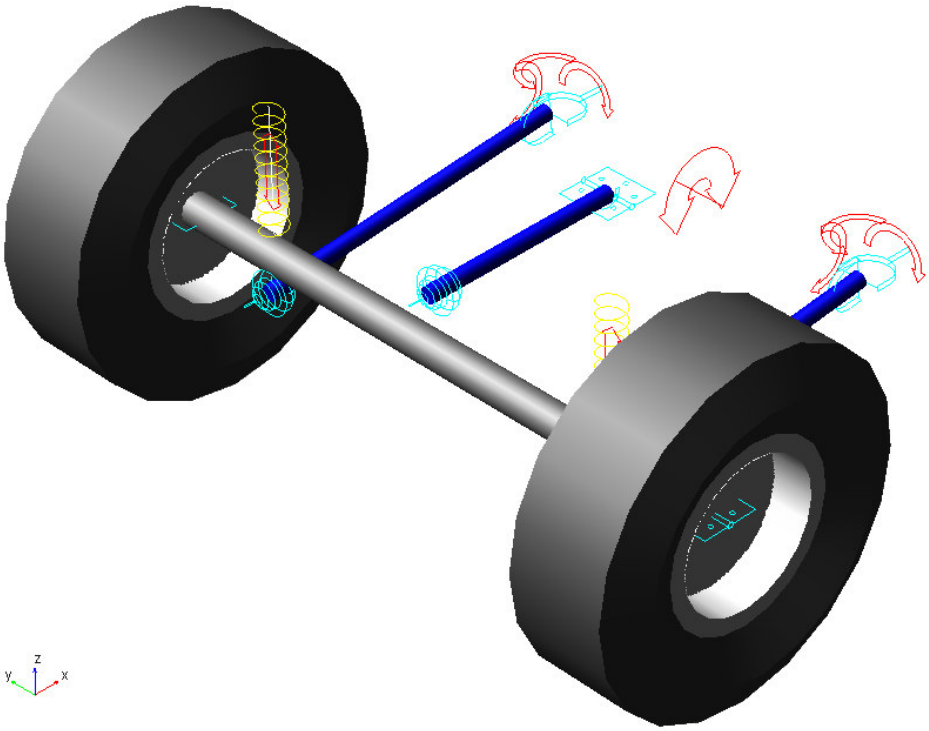

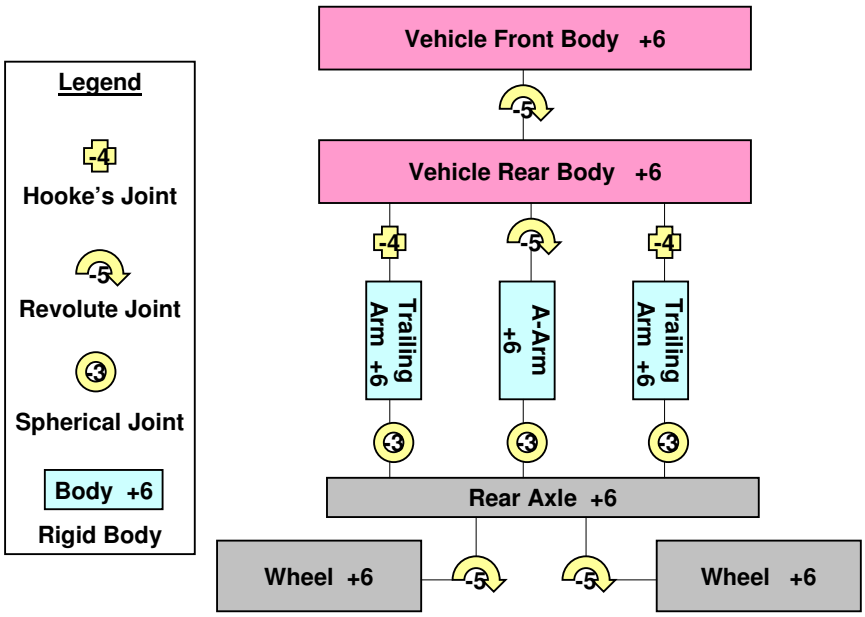

Figure 3.2: Modelling of the full vehicle in MSC.ADAMS, rear suspension

3.2.1 Validation of Full Vehicle Model

The MSC.ADAMS full vehicle model is validated against measured test results performed on the baseline vehicle. The measurement positions are defined by Figure 3.3 and Table 3.2. The correlation results are presented in Figure 3.4 for the baseline vehicle travelling over two discrete bumps to evaluate vertical dynamics, and in Figure 3.5 for the vehicle performing a double lane change manœuvre at 65 km/h. From the results it is evident that the model returns excellent correlation to the actual vehicle. It is, however, computationally expensive to solve and exhibits severe numerical noise due to all the included non-linear effects.

Table 3.2: Land Rover 110 test points

channel	point	position	measure	axis
1	B	center of gravity	velocity	longitudinal
2	G	left front bumper	acceleration	longitudinal
3				lateral
4				vertical
5	C	rear passenger	acceleration	longitudinal
6				lateral
7				vertical
8	I	right front bumper	acceleration	vertical
9	A	steering arm	displacement	relative arm/body
10	D	left rear spring	displacement	relative body/axle
11	E	right rear spring		
12	F	left front spring		
13	H	right front spring		
14	B	center of gravity	angular velocity	roll
15				pitch
16				yaw

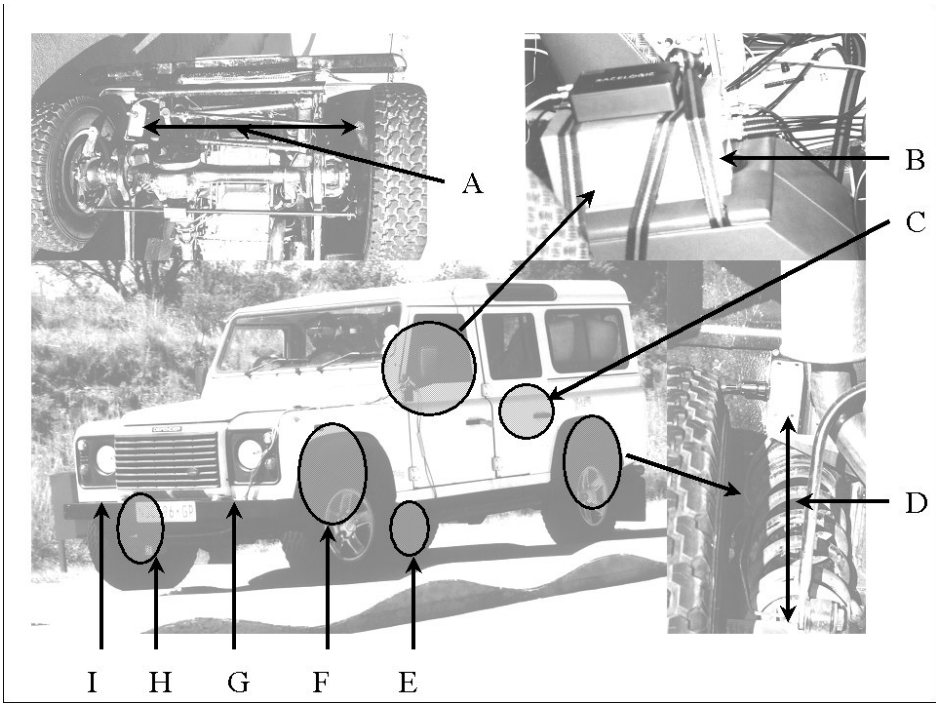

Figure 3.3: Test vehicle indicating measurement positions

3.3 Vehicle Speed Control

The speed control is modelled as a variable force F_{drive} attached to the body at wheel center height. The magnitude of this force depends on the difference between the instantaneous speed $\dot{x}_{act}$ and desired speed $\dot{x}_d$. Because the vehicle is a four-wheel drive with open differentials, the vertical tyre force $F_{z_{tyre}}$ is measured at all tyres (1 to 4). If a tyre looses contact with the ground, the driving force to the vehicle is removed until all wheels are again in contact with the ground. The driving force is thus defined as:

$$\begin{aligned} if \quad & F_{z_{tyre}1\rightarrow4} = 0 \\ & F_{drive} = 0 \\ & else \\ F_{drive} &= 4\frac{min(1200, 1200(\dot{x}_d - \dot{x}_{act}))}{0.4} \\ & end \end{aligned} \tag{3.1}$$

The gain value of 1200 was determined to be sufficiently large to ensure fast stable acceleration of the vehicle model from rest up to the desired simulation speed. This force is multiplied by 4 as there is one force acting on

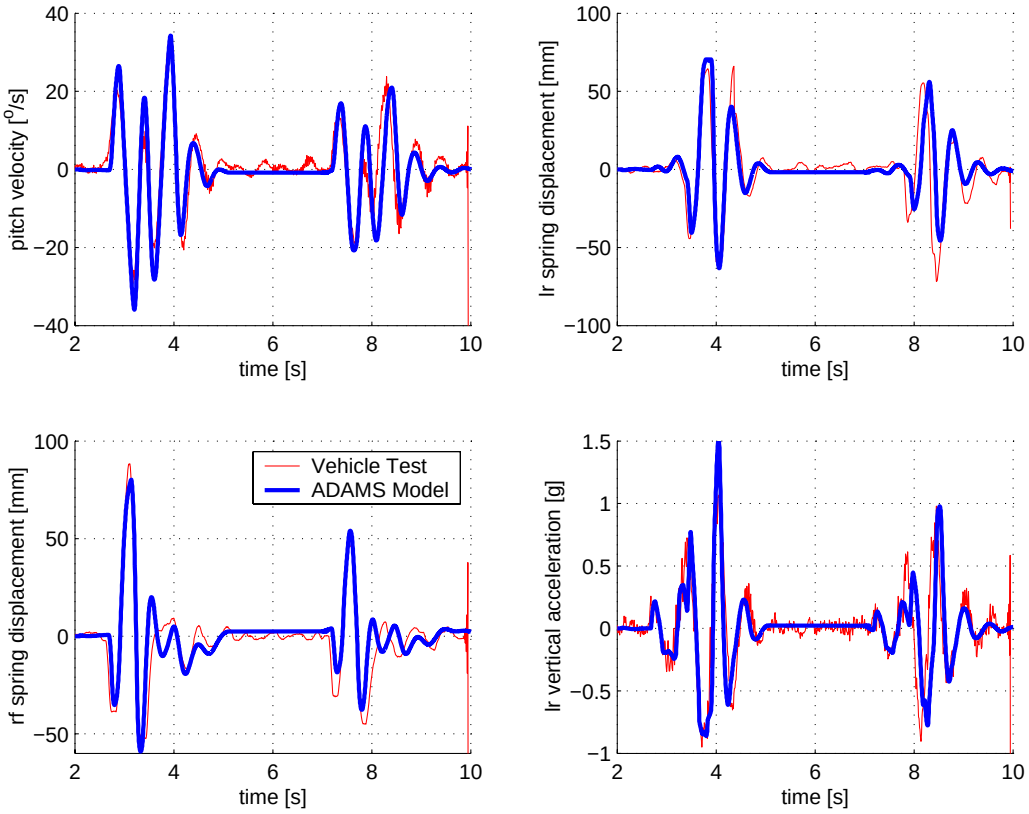

Figure 3.4: Discrete bumps, 15 km/h, validation of MSC.ADAMS model's vertical dynamics

the vehicle representative of the torque applied to the four wheels, and 0.4 meters is the radius of the tyres. The MSC.ADAMS model is then linked to the Simulink (Mathworks 2000b) based driver model that returns as outputs the desired vehicle speed and steering angle, calculated using the vehicle's dynamic response.

3.4 Driver Model For Steering Control

The use of driver models for the simulation of closed loop vehicle handling manœuvres is vital. However, great difficulty is often experienced in determining the gain parameters for a stable driver at all speeds, and vehicle parameters. A stable driver model is of critical importance during mathematical optimisation of vehicle spring and damper characteristics for handling, especially when suspension parameters are allowed to change over a wide range. The determination of these gain factors becomes

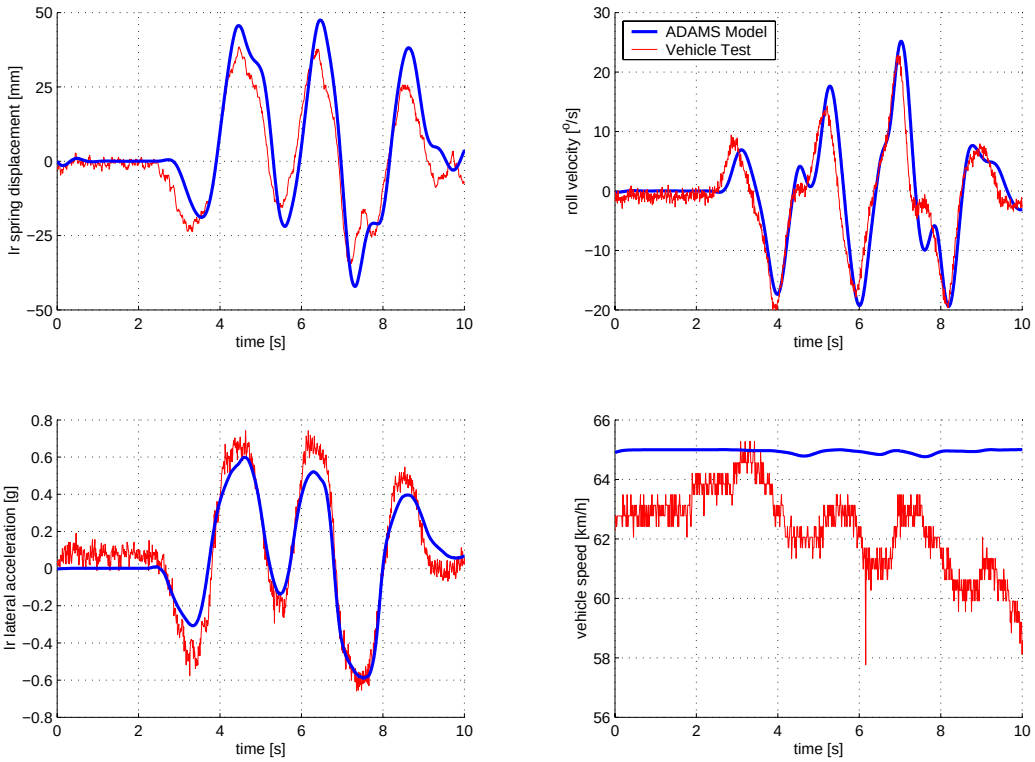

Figure 3.5: Double lane change, 65 km/h, validation of MSC.ADAMS model's handling dynamics

especially complex when accurate full non-linear vehicle models, with large suspension travel, are to be controlled. Single point preview models are normally unstable for such non-linear vehicle models. This paragraph investigates the relationship between vehicle yaw response and non-linear tyre characteristics. The non-linearity of the tyre characteristics is replicated for the steering gain parameter, ensuring the feasibility of single point preview models. This paragraph proposes the fitting of the Magic Formula, usually used for tyre modelling, to the non-linear response of the vehicle's yaw acceleration vs. steering velocity in terms of vehicle speed. The subject of the Magic Formula is reformulated, and used to determine the required steering input, for a given vehicle speed and desired yaw acceleration. The proposed steering driver is applied to the refined non-linear full vehicle model of a Sports Utility Vehicle (see paragraph 3.2), performing a severe double lane change manœuvre, and simulation results are compared to measured results. It is concluded that the proposed driver has definite merit, with

excellent correlation to test results.

The primary reason for requiring a driver model in the present study, is for the optimisation of the vehicle's suspension system. The suspension characteristics are to be optimised for handling, while performing the closed loop ISO3888-1 (1999) double lane change manœuvre. The driver model thus has to be robust for various suspension setups, and perform only one simulation to return the objective function value. Thus steering controllers with learning capability will not be considered, as the suspension could be vastly different from one simulation to the next. Only lateral path following is considered in this preliminary research, as the double lane change manœuvre is normally performed at a constant vehicle speed.

Previous research into lateral vehicle model drivers, was conducted amongst others by Sharp et al. (2000) who implement a linear, multiple preview point controller, with steering saturation limits mimicking tyre saturation, for vehicle tracking. The vehicle model used is a 5-degree-of-freedom (dof) model, with non-linear Magic Formula tyre characteristics, but no suspension deflection. This model is successfully applied to a Formula One vehicle performing a lane change manœuvre. Also Gordon et al. (2002) make use of a novel method, based on convergent vector fields, to control the vehicle along desired routes. The vehicle model is a 3-dof vehicle, with non-linear Magic Formula tyre characteristics, but with no suspension deflection included. The driver model is successfully applied to lane change manœuvres.

The primary similarity between these methods is that vehicle models with no suspension deflection were used. The current research is, however, concerned with the development of a controllable suspension system for Sports Utility Vehicles (SUV's). The suspension system thus has to be modelled, and the handling dynamics simulated for widely varying suspension settings. The vehicle in question has a comparatively soft suspension, coupled to a high center of gravity, resulting in large suspension deflections when performing the double lane change manœuvre. This large suspension deflection, results

in highly unstable vehicle behaviour, eliminating the use of driver models suited to vehicles with minimal suspension deflection. Steady state rollover calculations also show that the vehicle will roll over before it will slide.

Proköp (2001) implements a PID (Proportional Integral Derivative) prediction model for tracking control of a bicycle model vehicle. The driver model makes use of a driver plant model that is representative of the actual vehicle. The driver plant increases in complexity to perform the required dynamic manœuvre, from a point mass to a four wheel model with elastokinematic suspension. This model is then optimised with the SQP (Sequential Quadratic Programming) optimisation algorithm for each time step. This approach, however, becomes computationally expensive, when optimisation of the vehicle's handling is to be considered.

For the current research several driver model approaches were implemented, but with limited success. Due to the difficulty encountered with the implementation of a driver model for steering control, it was decided to characterize the whole vehicle system, using step steer, and ramp steer inputs, and observe various vehicle parameters. This lead to the discovery that the relationship between vehicle yaw acceleration vs. steering rate for various vehicle speeds appeared very similar to the side force vs. slip angle characteristics of the tyres. With this discovery it was decided to implement the proposed novel driver model, with the non-linear gain factor modelled with the Pacejka Magic Formula, normally used for tyre data.

3.4.1 Driver Model Description

To investigate the relationship between vehicle response and steering inputs, simulations were performed for various steering input rates (Figure 3.6, where t_s is the start of the ramp when the vehicle has reached the desired speed), at various vehicle speeds. It was found that there existed a trend very similar to the tyre's lateral force vs. slip angle at various vertical loads, (Figure 3.7) with the vehicle's yaw acceleration vs. steering rate at different vehicle

speeds (Figure 3.8). Because of this relationship it was postulated that the vehicle could be controlled by comparing the actual yaw acceleration to the desired yaw acceleration, and adjusting the steering input rate.

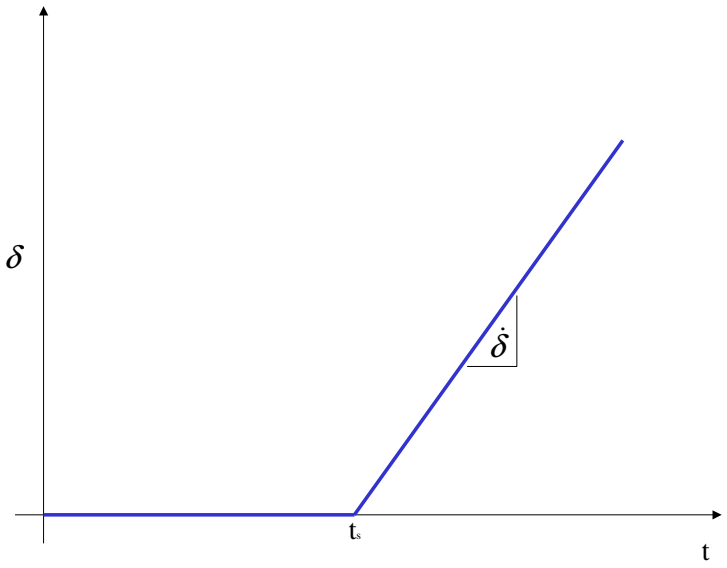

Figure 3.6: Vehicle characterisation steering input

From dynamics principles it is known that, for a rigid body undergoing motion in a plane, the rotational angle as a function of time is dependant on: the current rotational angle ϑ_0, the current rotational velocity $\dot{\vartheta}$, the rotational acceleration $\ddot{\vartheta}$, and the time step δt over which the rotational acceleration is assumed constant. If the rotational acceleration is not constant, but sufficiently small time steps are considered, the predicted rotational angle ϑ_p will be sufficiently well approximated. The predicted rotational angle can be determined as follows:

$$\vartheta_p = \vartheta_0 + \dot{\vartheta}\delta t + \frac{1}{2}\ddot{\vartheta}\delta t^2 \tag{3.2}$$

The above equation can be modified for a vehicle's yaw rotation motion by defining ϑ as the yaw angle ψ. Considering Figure 3.9, the driver model parameters can now be defined as:

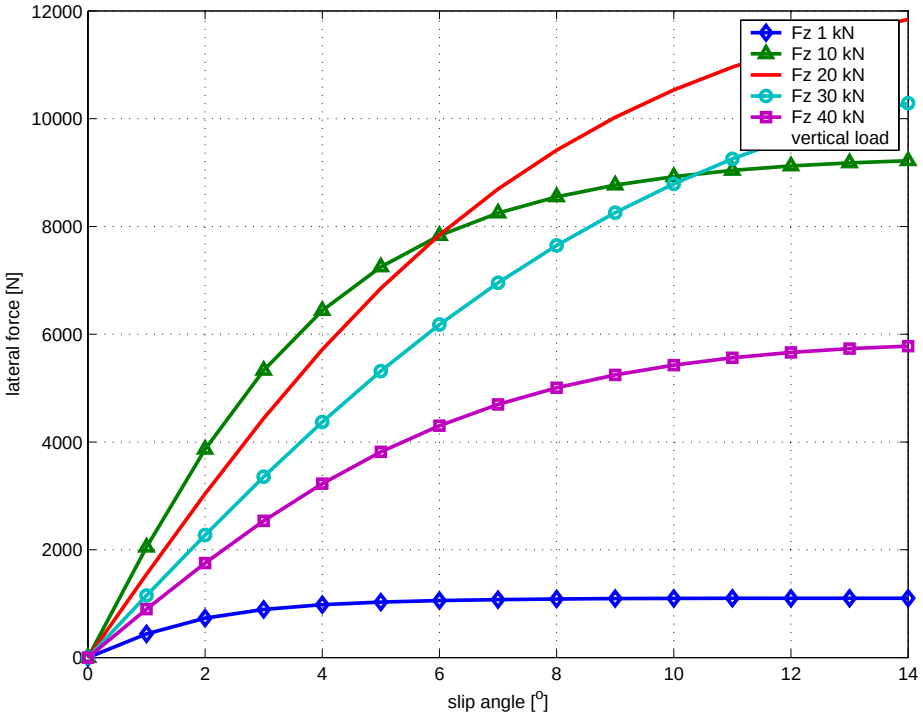

Figure 3.7: Tyre's lateral force vs. slip angle characteristics for different vertical loads

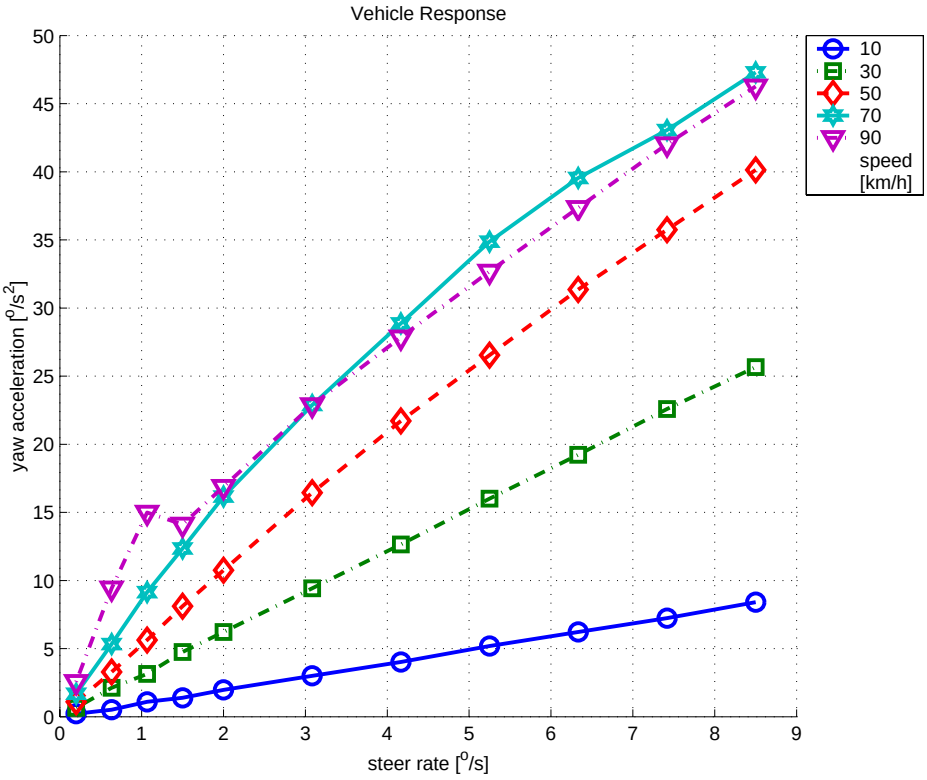

Figure 3.8: Vehicle yaw acceleration response to different steering rate inputs

- desired yaw angle of the vehicle ψ_d, equivalent to ϑ_p
- actual vehicle yaw angle ψ_a, equivalent to ϑ_0
- actual vehicle yaw rate $\dot{\psi}_a$, equivalent to $\dot{\vartheta}$
- response/preview time τ, equivalent to δt
- vehicle forward velocity $\dot{x}$

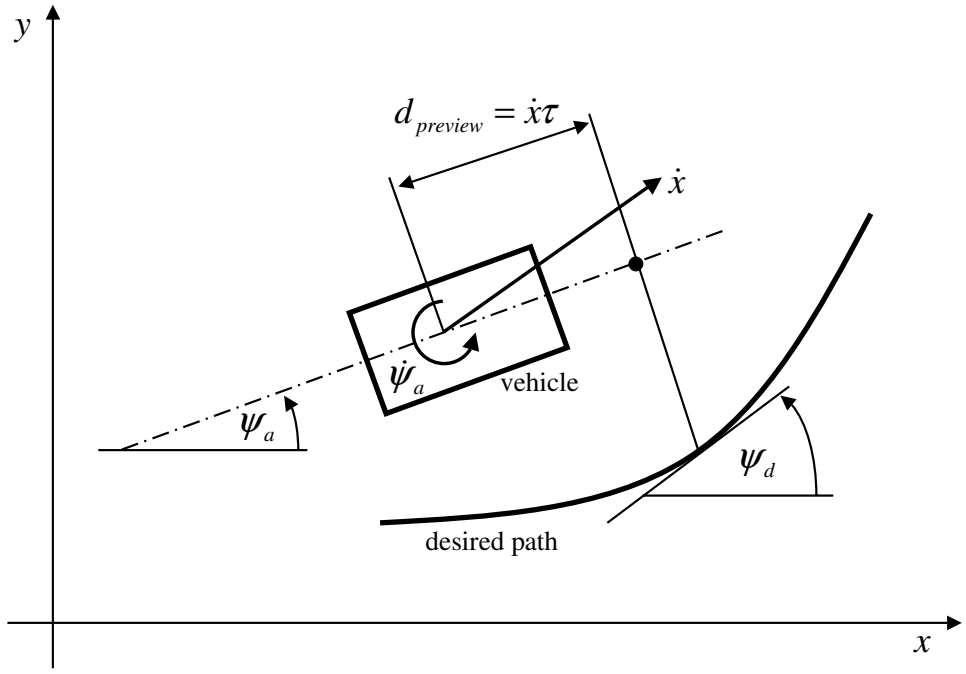

Figure 3.9: Definition of driver model parameters

The yaw acceleration $\ddot{\psi}$ needed to obtain the desired yaw angle is calculated from equation (3.2), substituting in the equivalent variables, as follows:

$$\ddot{\psi} = 2\frac{\psi_d - \psi_a - \dot{\psi}_a\tau}{\tau^2} \tag{3.3}$$

The vehicle's steady state yaw acceleration $\ddot{\psi}$ with respect to different steering rates $\dot{\delta}$, was determined for a number of constant vehicle speeds $\dot{x}$ and is presented in Figure 3.8. Where the vehicle's response did not reach steady-state, and the vehicle slided out, or rolled over, the yaw acceleration just prior to loss of control was used. This process is computationally

expensive as 11 different steering ramp rates, for each vehicle speed, were applied to the vehicle model and simulated. The steady state yaw acceleration reached was then used to generate the figure. When comparing Figure 3.8 to the vehicle's lateral tyre characteristics, presented in Figure 3.7, it appears reasonable that the Magic Formula could also be fitted to the steering response data. Therefore the reformulated Magic Formula, discussed below, is fitted to this data, and returns the required steering rate $\dot{\delta}$, which is defined as:

$$\dot{\delta} = f(\ddot{\psi}, \dot{x}) \tag{3.4}$$

As output, the driver model provides the required steering rate $\dot{\delta}$, which is then integrated for the time step δt to give the required steering angle δ.

The Magic Formula is fitted through the obtained data, as it is a continuous function over the fitted range. Normal polynomial curve fits would be discreet for the vehicle speed they are fitted to and an interpolation scheme would be necessary for in-between vehicle speeds. The Magic Formula is thus a continuous approximation described by 12 values, as opposed to multiple curve formulae, requiring intermediate interpolation.

3.4.2 Magic Formula Fits

The Magic Formula was proposed by Bakker et al. (1989) to describe the tyre's handling characteristics in one formula. In the current study the Magic Formula will be considered in terms of the tyre's lateral force vs. slip angle relationship, which directly affects the vehicle's handling and steering response. The Magic Formula is defined as:

$$\begin{aligned} y(x) &= Dsin(Carctan\{Bx - E(Bx - arctan(Bx))\}) \\ Y(X) &= y(x) + S_v \\ x &= X + S_h \end{aligned} \tag{3.5}$$

The terms are defined as:

- $Y(X)$ tyre lateral force F_y
- X tyre slip angle α

- B stiffness factor
- C shape factor
- D peak factor
- E curvature factor
- S_h horizontal shift
- S_v vertical shift

These terms are dependent on the vertical tyre load F_z and camber angle γ. The lateral force F_y vs. tyre slip angle α relationship typically takes on the shape as indicated in Figure 3.7, for different vertical loads. Considering the shape of Figure 3.8 presenting the yaw acceleration vs. steering rate for different vehicle speeds, the Magic Formula can be successfully fitted, with the parameters redefined as:

- vertical tyre load F_z is equivalent to vehicle speed $\dot{x}$
- tyre slip angle α is equivalent to steering rate $\dot{\delta}$
- tyre lateral force F_y is equivalent to vehicle yaw acceleration $\ddot{\psi}$

The Magic Formula for the vehicle's steering response can now be stated as:

$$\begin{aligned} y(x) &= Dsin(Carctan\{Bx - E(Bx - arctan(Bx))\}) \\ Y(X) &= y(x) + S_v \\ x &= X + S_h \end{aligned} \tag{3.6}$$

With the terms defined as:

- $Y(X)$ yaw acceleration $\ddot{\psi}$
- X steering rate $\dot{\delta}$
- B stiffness factor
- C shape factor
- D peak factor

- E curvature factor
- S_h horizontal shift
- S_v vertical shift

With the redefined parameters, the Magic Formula coefficients can be determined in the usual manner. The determination of the coefficients applied for the steering driver is now discussed. The baseline vehicle's response as indicated in Figure 3.8 is used for the fitting of the parameters.

3.4.3 Determination of Factors

The peak factor D is determined by plotting the maximum yaw acceleration value $\ddot{\psi}$ against the vehicle speed $\dot{x}$. For this the graphs have to be interpolated. Quadratic curves were fitted through the vehicle's response curves, and the estimated peak values were used. The peak factor is defined as:

$$D = a_1\dot{x}^2 + a_2\dot{x} \tag{3.7}$$

The peak factor curve was fitted through the estimated peak values, with emphasis on accurately capturing the data for vehicle speeds of 50 to 90 km/h. The 90 km/h peak was taken as the point where the graph changed due to the maximum yaw acceleration just prior to roll-over. The resulting quadratic curve fit to the predicted peak values of the yaw acceleration is shown in Figure 3.10. It is observed that the fit for the Magic Formula is poor for 30 km/h. This is attributed to the almost linear curve fit through the yaw acceleration vs. steering rate for speeds of 10 and 30 km/h Figure 3.6, resulting in an unrealistically high prediction of the peak values.

In the original paper (Bakker et al. 1989), BCD is defined as the cornering stiffness, here it will be termed the 'yaw acceleration gain'. For the yaw acceleration gain the gradient at zero steering rate is plotted against vehicle speed as illustrated in Figure 3.11. The camber term γ of the original paper will be ignored so that coefficient a_5 becomes zero. The yaw acceleration gain is fitted with the following function:

$$BCD = a_3 sin(2arctan(\dot{x}/a_4))(1 - a_5\gamma) \tag{3.8}$$

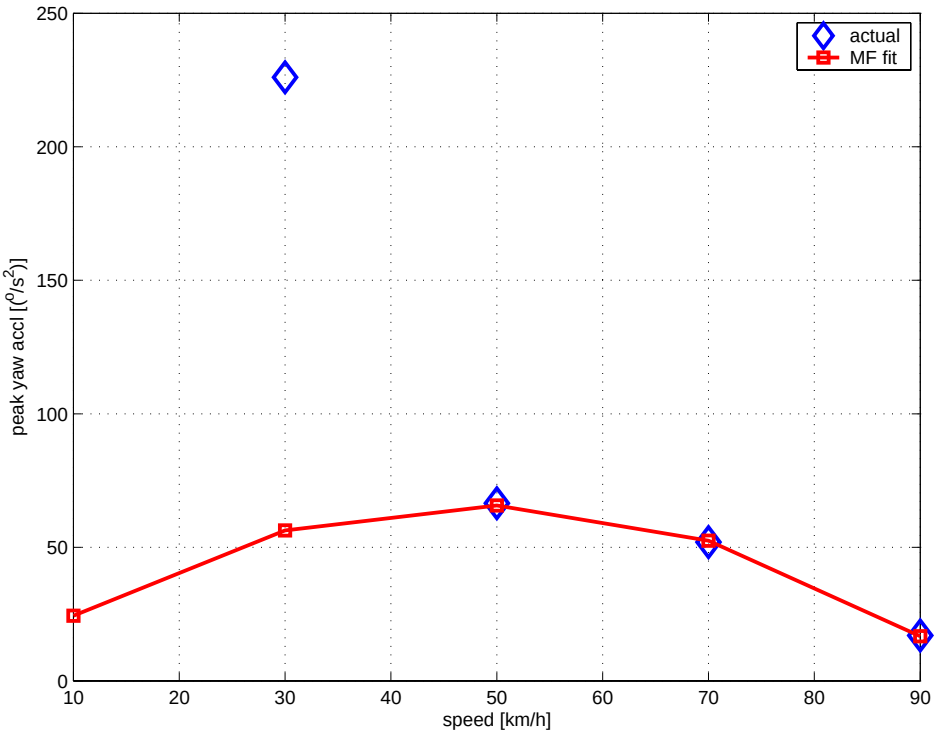

Figure 3.10: Magic Formula coefficient quadratic fit through equivalent peak values

For the determination of the curvature E, quadratic curves were fitted through each of the curves in Figure 3.8. These approximations could then be differentiated twice to obtain the curvature for each. This curvature is plotted against vehicle speed $\dot{x}$, and the straight line approximation:

$$E = a_6\dot{x} + a_7 \tag{3.9}$$

is then fitted through the data points, in order to determine the coefficient a_6 and a_7. The straight line approximation fitted through the points is shown in Figure 3.12.

The shape factor C, is determined by optimising the resulting Magic Formula fits to the measured data. This parameter is the only parameter that has to be adjusted in order to achieve better Magic formula fits to the original

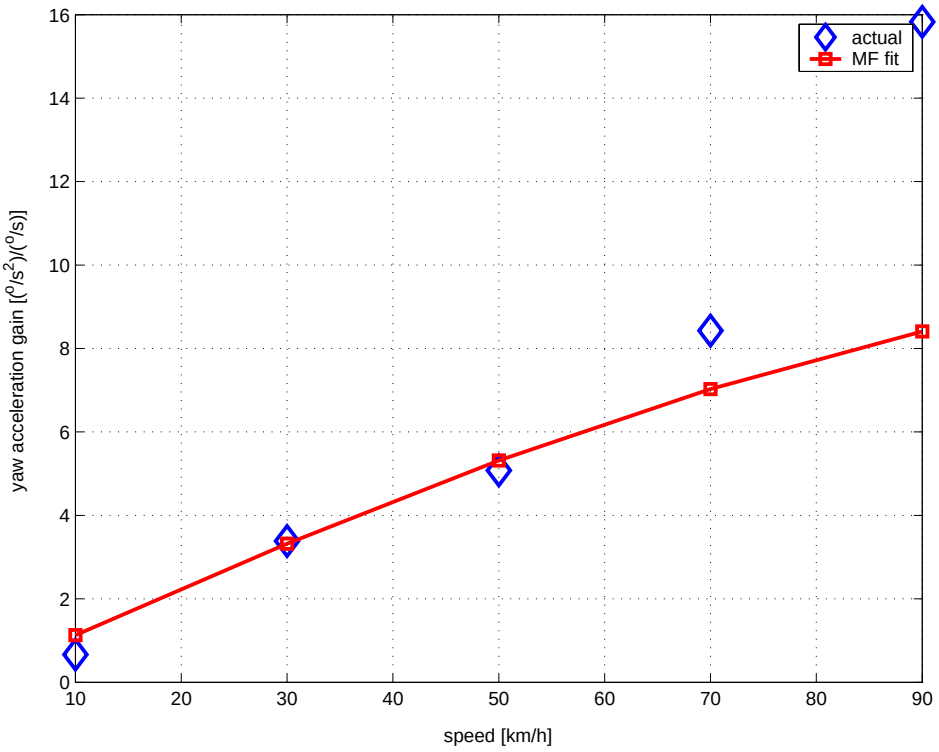

Figure 3.11: Magic Formula fit of yaw acceleration gain through the actual data

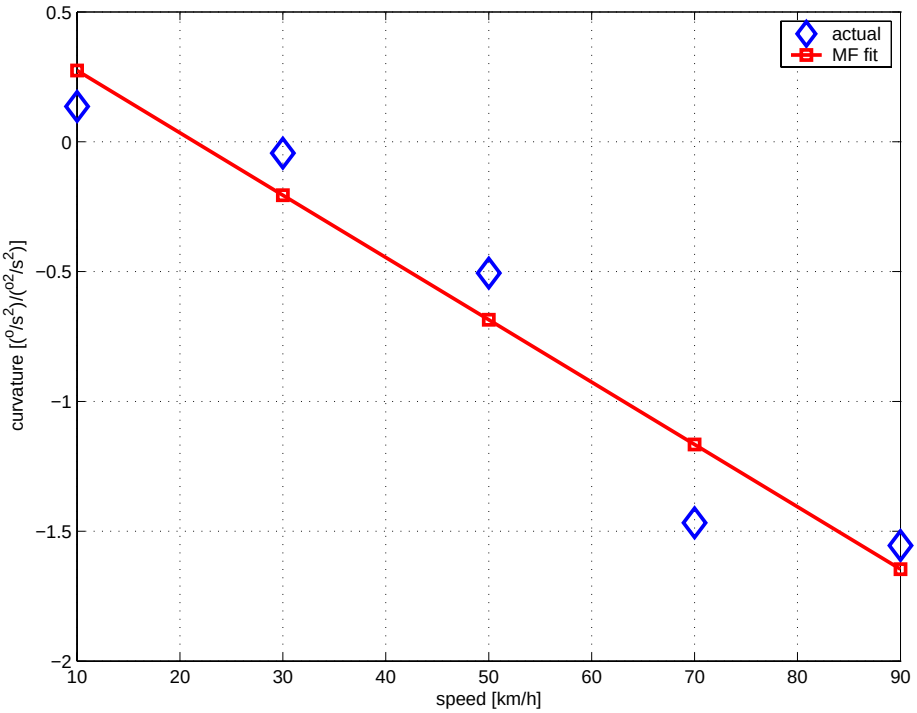

Figure 3.12: Determination of curvature coefficients

data. It is defined in terms of the Magic Formula coefficient a_0 as follows:

$$C = a_0 \tag{3.10}$$

The stiffness factor B is determined by dividing BCD by C and D:

$$B = BCD/CD \tag{3.11}$$

In the current research the horizontal and vertical shift of the curves were ignored allowing coefficients a_8 to a_{13} to be assumed zero. The Magic Formula fits to the original data are presented in Figure 3.13. It can be seen that most of the fits except for 90 km/h are very good. The vehicle simulation failed for most of the steering rate inputs before reaching a steady state yaw acceleration at 90 km/h, thus this can be viewed as an unstable regime. With the Magic formula coefficients being determined, the manipulation of the Magic formula for the driver application is discussed.

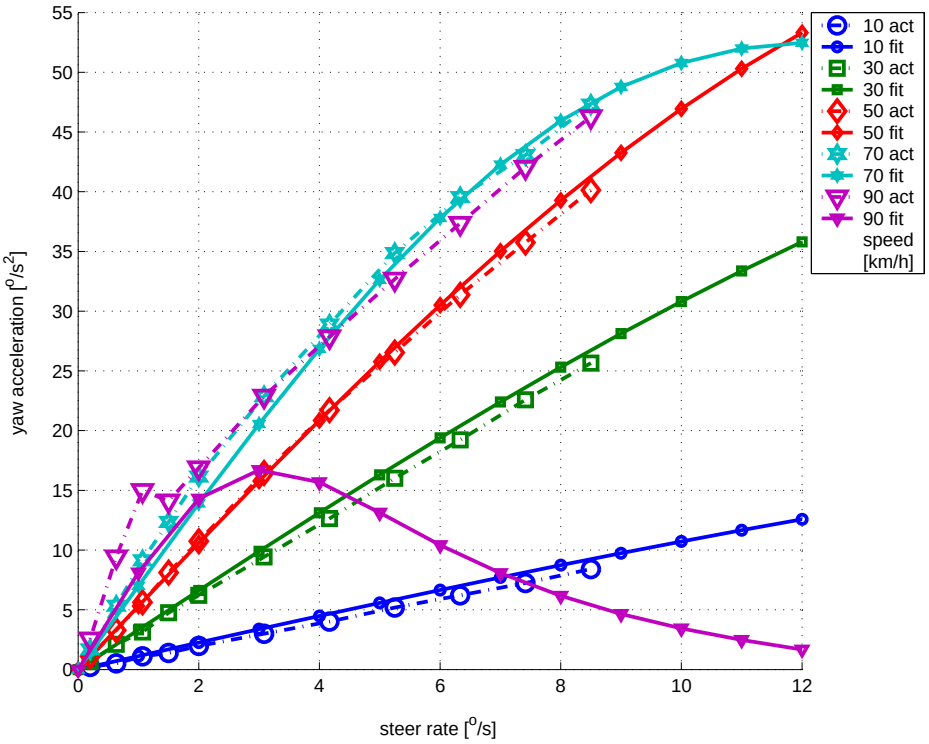

Figure 3.13: Magic Formula fits to original vehicle steering behaviour

3.4.4 Reformulated Magic Formula

The steering driver requires, as output, the steering rate $\dot{\delta}$. For this reason the Magic Formula's subject of the formula must be reformulated, to make

it possible to have as inputs, vehicle velocity $\dot{x}$ and required vehicle yaw acceleration $\ddot{\psi}$, and as output required steering rate $\dot{\delta}$. However, due to the nature of the Magic Formula it is not possible to change the subject of the formula, so the *arctan* function is described by the *pseudo arctan* function as suggested by Pacejka (2002) as:

$$psatan(x) = \frac{x(1 + a\,|x|)}{1 + 2(b\,|x| + ax^2)/\pi} \tag{3.12}$$

where $a = 1.1$ and $b = 1.6$. The Magic Formula can now be written as:

$$F = Bx - E\left(Bx - \frac{Bx(1+a|Bx|)}{1+2(b|Bx|+a(Bx)^2)/\pi}\right)$$
$$F = tan\left(\frac{arcsin(\frac{y}{D})}{C}\right) \tag{3.13}$$

This equation was solved symbolically for x using MATLAB's Symbolic Toolbox, and returns an exceptionally long equation, of three terms, not presented here due to its shear size. This resulting equation is coded into the Simulink model consisting of the MSC.ADAMS model and the steering controller. It should be noted that the solution to equation (3.13) will return multiple answers as the shape of the graphs in Figure 3.13 suggest. Only the first part of the graphs, up to the peak/maximum point, was used, with the peak point used as a limit for higher steering rates.

3.4.5 Implementation of Results

In order to validate the performance of the proposed methodology, the Magic Formula driver was implemented in the vehicle simulation model. The vehicle was simulated performing the ISO3888-1 (1999) double lane change manœuvre. The excellent comparison to measured results is presented in Figure 3.14, for kingpin steering angle, yaw velocity, left rear (lr) spring displacement and left front (lf) lateral acceleration. It is important to note that the double lane change is simulated at a constant speed (see results in Figure 3.5) while the measured results show that the driver decreased speed during the manœuvre, explaining the slight discrepancies towards the end of the double lane change.

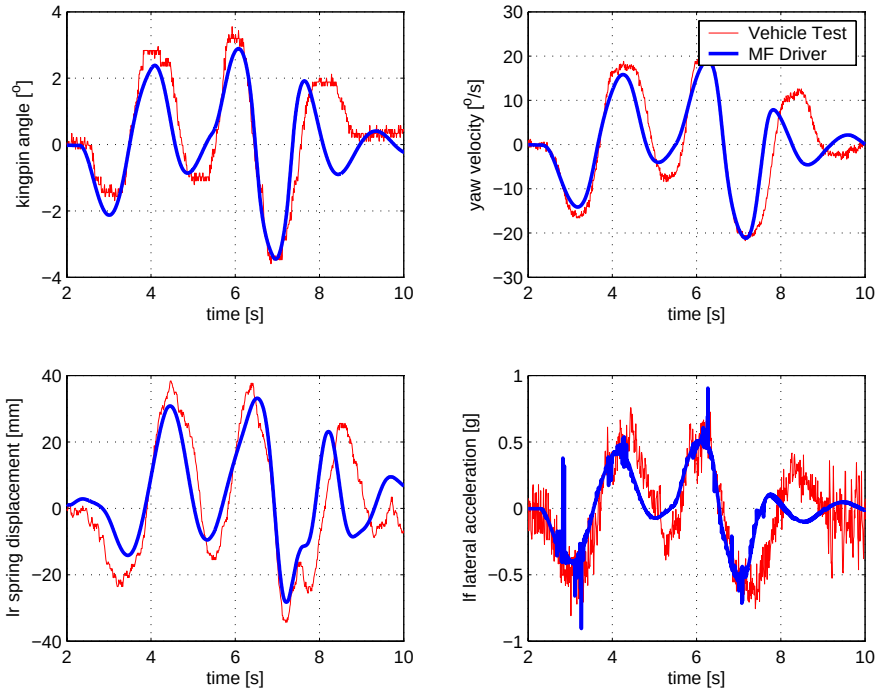

Figure 3.14: Correlation of Magic Formula driver model to vehicle test at an entry speed of 63 km/h

The driver model was then analysed for changing the vehicle's suspension system from stiff to soft, for various speeds. Presented in Figure 3.15 is the driver model's ability to keep the vehicle at the desired yaw angle (Genta 1997) over time. From the results it can be seen that a varying preview time with vehicle speed, would be beneficial, however, it is felt that for this preliminary research the constant 0.5 seconds preview time is sufficient. Also it is evident that the softer suspension system, and 70 km/h vehicle speed, are slightly unstable, as seen by the oscillatory nature at the end of the double lane change manœuvre.

The results show that the driver model provides a well controlled steering input. Also there is a lack of high frequency oscillation typically associated with single point preview driver models, when applied to highly non-linear vehicle models like SUV's, that are being operated close to their limits in the

double lane change manœuvre.

3.5 Conclusions

It has been shown that the Magic Formula, traditionally used for describing tyre characteristics, can be fitted to the vehicle's steering response, in the form of yaw acceleration vs. steering rate, for different vehicle speeds.

A single point steering driver model has been successfully implemented on a highly non-linear vehicle model. The success of the driver model, is attributed to the modelling of the vehicle's response with the Magic Formula. The success of the single point steering driver can be related to the non-linear gain factor, that changes in value with vehicle speed and required yaw acceleration.

Future work should entail an investigation into determining the parameters of the vehicle that modify the tyre characteristic Magic Formula coefficients to arrive at the steering rate and yaw acceleration parameters. Ideally the tyre Magic Formula coefficients should be multiplied by some modifying factor, based on vehicle characteristics, to be used directly for the control of the vehicle steering. This would eliminate the need for the computationally expensive characterisation currently required. A further aspect that could be considered is determining the value of varying preview time with vehicle speed. The driver model is, however, sufficiently robust to be used in the optimisation of the vehicle's suspension characteristics for handling.

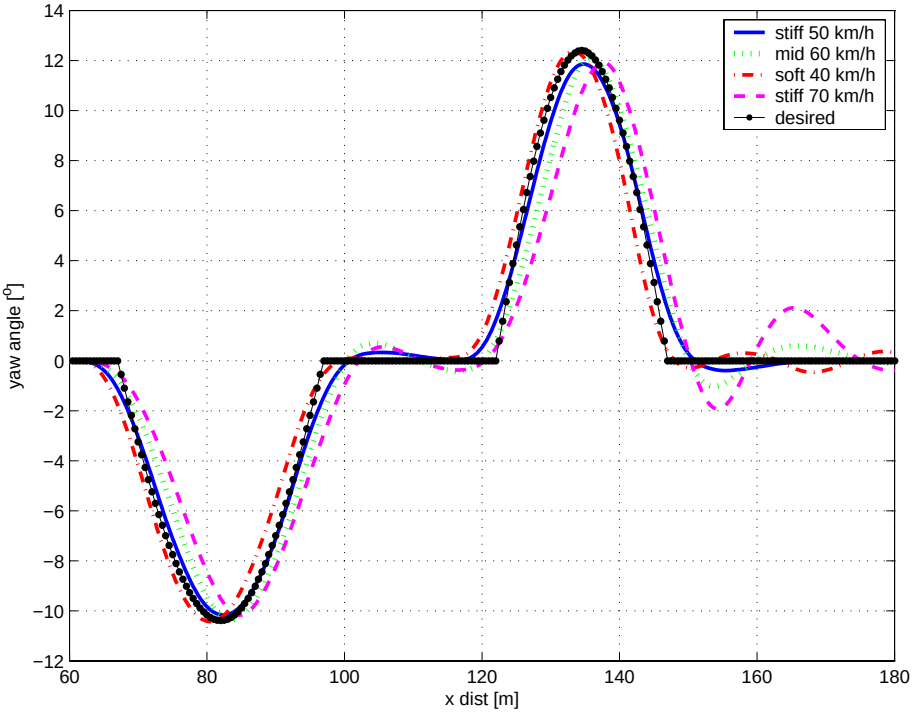

Figure 3.15: Comparison of different suspension settings and vehicle speeds, for the double lane change manœuvre, where the desired is as proposed by Genta (1997)